



Title	High-speed spectroscopic OCT around 1550 nm based on dual-band swept laser source
Author(s)	Zhu, R; Xu, J; Zhang, C; Lam, EYM; Wong, KKY
Citation	SPIE Photonics West, San Francisco, CA., 21-26 January 2012. In Proceedings of SPIE, 2012, v. 8213, p. 82132O-1-82132O-7
Issued Date	2012
URL	http://hdl.handle.net/10722/160267
Rights	Proceedings of SPIE. Copyright © SPIE - International Society for Optical Engineering.

High-speed spectroscopic OCT around 1550 nm based on dual-band swept laser source

Rui Zhu^a, Jianbing Xu^a, Chi Zhang^a, Edmund Y. Lam^a and Kenneth K.Y. Wong^a

^aDepartment of Electrical and Electronic Engineering, The University of Hong Kong, Pokfulam Road, Hong Kong

ABSTRACT

We report a 45 kHz spectroscopic OCT system based on a swept laser source utilizing two wavelength bands. The source is generated by single-band swept laser input and a fiber optical parametric amplifier. The time-multiplexing architecture reduces the complexity of the coupling and detecting configuration in comparison with the previous dual-band swept-source setup. This high-speed spectroscopic OCT combines the advantages of the speed of the swept laser and contrast enhancement, in comparison with the time or spectral-domain spectroscopic OCT system. In the experiment, spectroscopic OCT imaging around 1550 nm is achieved for the first time. The difference in images at 1500 nm and 1600 nm clearly shows different back scattering and penetration properties which can be used for tissue classification and water content measurement.

Keywords: Swept source, optical coherence tomography (OCT), spectroscopic imaging, fiber optical parametric amplification (OPA), dual-band source

1. INTRODUCTION

As a noninvasive imaging modality, optical coherence tomography (OCT) has been widely studied in biomedical research and clinical diagnosis fields. OCT uses broadband light to achieve spatial resolutions approaching the cellular level. Basic OCT technology provides cross-sectional structural information by demodulating the depth dependent correlation signals. With combination of different technologies such as Doppler shift analysis, microscopy, and spectral analysis, many functional methods have been developed, which greatly extend the applications of OCT. One of the branches known as spectroscopic OCT (SOCT) has been demonstrated to be a powerful tool for the classification of different tissue types.¹ Additional imaging contrast is achieved by the spatial mapping of spectral characteristics onto the structural images.

In a time-domain OCT (TD-OCT) system, the spectral information is evaluated by a time-frequency analysis of the correlation signal. The algorithm is complicated and computationally expensive. After development of Fourier domain OCT, a two-spectrometer-based system is employed to synchronously detect signals from two distinct wavelength bands.² However, it has a speed of up to 1.1k axial scans per second which is limited by the low readout rates of the infrared camera. The frequency swept laser has recently enabled imaging speeds of up to millions of axial scans per second.³ The drawbacks of a conventional swept-source laser such as low power, increased amplitude noise and broad instantaneous linewidth under high scan rate are overcome with the help of Fourier domain mode locking (FDML) technology. A FDML swept laser can dramatically improve the sweep rate while maintaining high power and narrow linewidth. To further increase imaging speed in spectroscopic OCT, it is essential to build a dual-band system based on FDML swept-source.

Current FDML lasers only produce sweeping in the signal wavelength band because the amplifiers such as the semiconductor optical amplifier (SOA) in the cavity can only be operated in certain wavelengths and usually the range is relatively limited. To extend the sweep range, innovative amplifying architectures should be considered. A suitable solution is provided by the fiber optical parametric amplifier (OPA). In OPA, the amplification wavelength can be arbitrarily chosen as long as the phase-matching conditions can be fulfilled. It can potentially provide a gain range of over 400 nm which is superior to SOA and Raman amplification,⁴ though

Further author information: (Send correspondence to Kenneth K. Y. Wong)
Kenneth K. Y. Wong: E-mail: kywong@eee.hku.hk, telephone: 852-28678483

its actual performance depends on fiber nonlinearity, pump power and fiber dispersion. Most importantly, the fiber OPA produces two wavelength regimes: signal and idler bands. It will replicate the original signal spectrum so that a new sweeping range in idler band can be generated directly. The nature of fiber OPA makes it an ideal choice for the dual-band swept-source.

In spectroscopic OCT, usually different wavelengths with different scattering, transmission and absorption characteristics are employed. Water absorption and photon backscattering are commonly used to identify the properties of tissue. In our setup the wavelength combination of 1500/1600 nm rather than 1550/1300 nm⁶ is chosen based on two reasons: (1) water absorption coefficient has a 10 dB difference for 1500/1600 nm combination. While for 1550/1300 nm combination, the difference is only 5 dB.⁷ Larger difference in the combination results in better contrast between OCT images of the two bands; (2) when applying OCT to clinical diagnosis, the bottleneck lies more in the penetration depth. OCT image around 1600 nm has been proved to enable better penetration depth in tissue in comparison with that at 1310nm.⁸ Therefore the dual-band combination around 1550 nm is believed to be more suitable for OCT imaging in tissue.

In this paper, we report a simultaneous 1500 and 1600 nm bands swept laser source based on the OPA. We launched a FDML laser source into a fiber OPA and then two wide sweeping bands are generated. With a time-delay module, the two synchronized swept lasers are separated and combined into a time-multiplexed manner which greatly simplifies the configuration in the OCT imaging part. The common-path dual-band swept laser for high speed SOCT is demonstrated with simultaneous imaging at 1500 and 1600 nm wavelength band.

2. PRINCIPLE

2.1 OPA based swept laser

Fiber OPA is based on the third-order nonlinear susceptibility of fibers. When a weak signal and strong pump power are fed into nonlinear gain medium such as a length of highly nonlinear fiber, an idler can be generated. The signal and idler will grow together if the pump is powerful enough, as well as the phase-matching conditions are satisfied. As an amplifier, fiber OPA is also proved to be a wide gain medium. Marhic et. al. demonstrated a pulsed fiber OPA with a gain in excess of 20 dB over 400 nm in a 30-m highly-nonlinear dispersion-shifted fiber (HNL-DSF).⁵ However, other experiment in which OPA was incorporated into FDML show that only a sweep range over 80 nm was realized within the cavity.⁹ Because of the FFP-TF, there is a threshold value (tens of mW) for the pump power inside. An excessive power may damage the fiber. As a result, in the swept laser cavity, even though the OPA itself enables a wide gain range, the practical amplified range is restricted to prevent component damage.

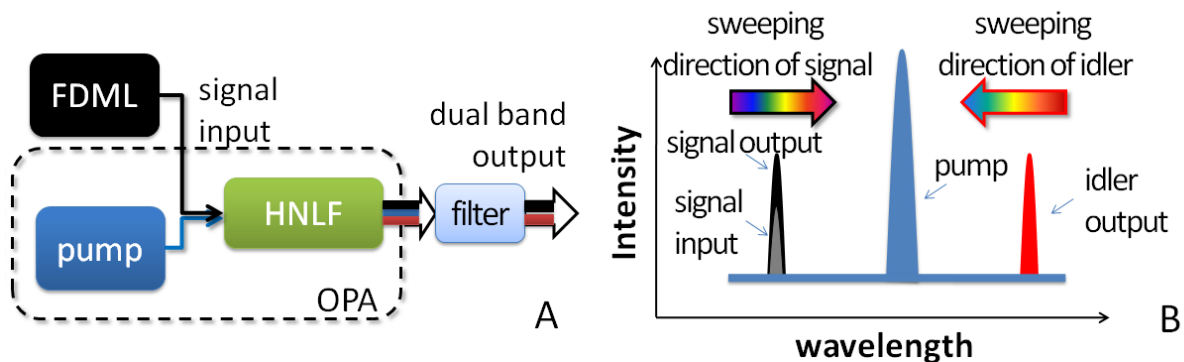


Figure 1. Schematic diagram of (A) the regime of OPA based dual-band swept-source; (B) the tuning and amplification of signal input and the corresponding tuning of the idler output around a fixed pump laser.

If OPA is set out of the cavity ring structure, the restriction on transmitted power will be removed. In the booster configuration, final output laser can maintain the coherence properties at the level of FDML. Fig. 1 shows the schematic diagram of the experimental setup for generating dual-band swept-source. When the FDML signal propagates with a CW pump through a nonlinear gain medium (e.g. HNL-DSF) for OPA, the signal is

amplified and a new wavelength component called idler is generated. As the signal FDML is wavelength swept, the corresponding idler band will also be wavelength swept as shown in Fig. 1(B). Therefore, after the OPA, a new wavelength swept idler band is generated.

3. DESIGN AND SETUP

3.1 Setup of the dual-band time-multiplexing swept laser

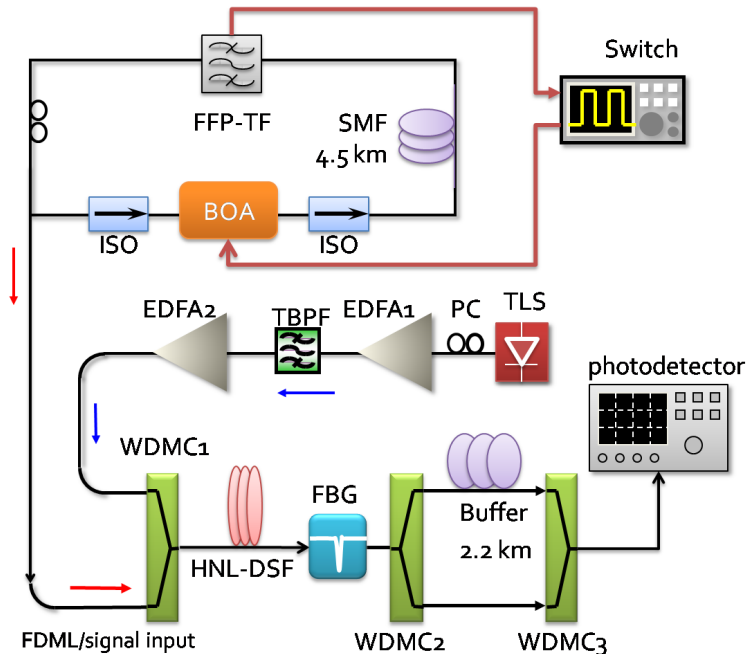


Figure 2. Setup of the dual-band time-multiplexing swept laser. FFP-TF: fiber Fabry-Perot tunable filter; SMF: single-mode fiber; BOA: boost semiconductor optical amplifier; EDFA: Erbium doped fiber amplifier; WDMC: wavelength-division multiplexer coupler; TBPF: tunable bandpass filter; PC: polarization controller; TLS: tunable laser source. HNL-DSF: highly-nonlinear dispersion-shifted fiber; FBG: fiber Bragg grating; PM: phase modulator.

Fig. 2 was a schematic diagram of the dual-band time-multiplexing swept laser. The signal band was generated from a standard FDML laser at 1500nm. The fiber ring cavity consisted of a SOA (BOA-1080S, Thorlabs) as a gain medium and a FFP-TF (Micron Optics) as the fast tunable bandpass filter. The BOA is polarization sensitive so that a polarization controller was inserted into the cavity to shape the output waveform. The FFP-TF has a free spectral range of 200nm at 1550 nm and a finesse of 1000. The fiber delay line (SMF28e, Corning) is 4.5 km long which corresponds to an operation frequency of 44 kHz. The fast switch was externally triggered by the TTL output from the driver (Micron Optics) of FFP-TF, to generate a synchronous square wave to control the BOA. A trigger delay can be adjusted to exactly cancel the back-forward sweep.

The FDML exports a power of 0.8 mW which was then combined with the high power continuous-wave (CW) pump at the WDM coupler. The CW pump was obtained from a tunable laser source followed by a two-stage Erbium-doped fiber amplifier (EDFA). A polarization controller was used to align the state-of-polarization (SOP) of the pump to the phase modulator (PM), in order to suppress the stimulated Brillouin scattering (SBS). The tunable bandpass filter was inserted between two EDFAs to suppress amplified spontaneous emission (ASE) noise. Both the sweeping signal band and high power CW pump were coupled into a 150-m HNL-DSF with a nonlinear coefficient of $14 \text{ W}^{-1}\text{km}^{-1}$ and zero-dispersion wavelength at 1554.7 nm. A length of 2.2-km SMF as the time-delay buffer is inserted between WDMC₂ and WDMC₃. The respective shift in time is prepared for the final combination. By this time-multiplexing method, the tailor-made laser output is generated and swept with different wavelength.

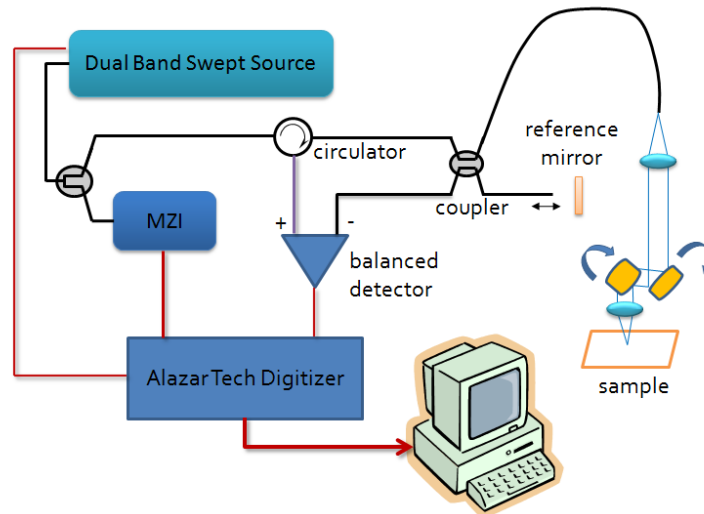


Figure 3. Schematic diagram of dual band swept source OCT. MZI: Mach-Zehnder Interferometer.

3.2 OCT imaging setup

Fig. 3 shows the schematic diagram of the OCT system. In comparison with the setup,⁶ only one set of coupling and detecting part is required. In addition, balanced detection is available in our setup which can improve the signal-to-noise ratio of by 6 dB. The output from time-multiplexing swept-source was connected to a 95/5 fiber beam splitter. 5% entered into a Mach-Zehnder interferometer (MZI) (INT-MZI-1550, Thorlabs) for calibration. The MZI has a free spectral range of 103 GHz. The sinusoidal fringe signal was acquired by a 12-bit precision digitizer card operating at up to 250 million samples per second (ATS9325, Alazar Tech). About 95% of the power from the source entered into a 50/50 fiber coupler that passed through a broadband circulator, which had a maximum of 1.5dB of signal loss. A reflected mirror that moves along a translation stage was placed at the reference end to search for the interference range. In the detection part, a balanced detector with a bandwidth of 100 MHz and a trans-impedance gain of 50,000 V/A is used to cancel background noise and enhance the amplitude by a factor of two. Calibration curves for two bands were prepared from the recorded MZI signal for resampling. The resampling and fast Fourier transform (FFT) procedures were performed by a graphical processing unit card (GTX460, NVIDIA) inserted into a standard personal computer (Dual core, Dell). Post-processed OCT images for the 1500 nm band and the 1600 nm band were produced. The two bands were color encoded and combined to form a single spectroscopic OCT image.

4. EXPERIMENTAL RESULTS

4.1 Power, spectra and sensitivity

The typical FDML laser has an output power of 0.5 mW centered at 1510 nm with a 60 nm bandwidth. The pump laser (1555 nm) was measured 2 W after the two-stage EDFA. After the pump was fed into HNL-DSF, an optical parametric gain of 16 dB was achieved. Considering a loss of 1.5 dB in the 150 m HNL-DSF coil, a total gain of 14.5 dB is obtained from OPA. OPA generates an idler with a bandwidth of 60 nm at 1600 nm as well. The pump wavelength had been filtered out by a fiber Bragg grating (FBG) filter. The spectra of the two bands after separated are shown in Fig. 4. The signal and idler bands are measured in each channel after WDM coupler. For signal band, due to the finite out-of-band suppression ratio of the WDM coupler, some power of idler leaks into the signal channel and results in the residual tail in the signal's spectrum between 1560 nm to 1620 nm. The tail is sweeping and detected simultaneously with the main part of signal band in 1480-1540 nm. Considering its power which is ~20 dB lower than the main part, the tail's influence as noise on the sensitivity of the signal band is negligible. A total swept-range of 140 nm is covered by the dual-band swept-source, which is only limited by the pump power. With special high-power fiber components, the system can tolerate a much

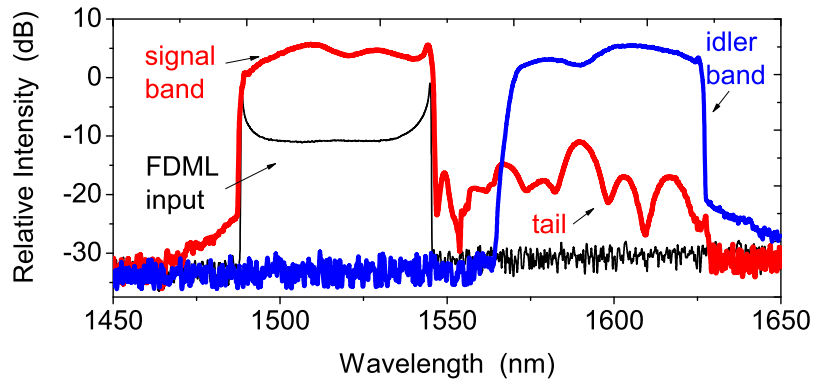


Figure 4. Integrated spectra of the dual-band source for two bands.

higher pump power and as a result the swept range will be further expanded. In addition to that, the fiber with higher nonlinearity can also enhance the range.

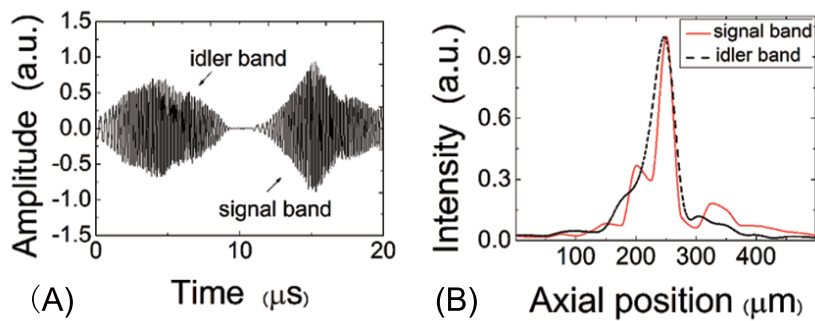


Figure 5. Interference fringes of (A) a magnification of the same data set showing a single sweep; (B) Point spread functions (PSF) of two bands. Axial resolution is measured $34 \mu\text{m}$ in signal band and $48 \mu\text{m}$ in idler band.

The output power levels of the signal and idler bands are 8.0 and 7.2 mW, respectively. After delayed in a 2.2 km buffer fiber and combined into time series by a WDM, the final averaged power of the dual-band swept-source was about 7 mW. Fig. 5(A) shows the interference fringes generated in the MZI. The patterns are easily influenced by the polarization state of the light from the FDML laser. A polarization controller before the WDM coupler was used to optimize the envelopes. Fig. 5 (B) shows the PSF function at two bands. In theory, the 60 nm bandwidth centered at 1520 nm and 1600 nm corresponds to a coherence length of $\sim 30 \mu\text{m}$ and $\sim 35 \mu\text{m}$, respectively. The measured values are $34 \mu\text{m}$ and $48 \mu\text{m}$. The slight degradation of the resolution at 1600 nm may inherit from the fluctuation of the polarization state. The detection sensitivity was measured using an attenuated, calibrated reflection from a mirror. The reference arm power was attenuated to less than a microwatt to avoid saturation in the detector. A sensitivity value of 85 dB and 84 dB for signal and idler respectively, was obtained. Fig. 6 shows the signal-to-noise ratio versus the depth at a 1500 nm signal and 1600 nm idler bands. At the 1500 nm band, the sensitivity drops by 6 dB at a depth of 4.1 mm, while at 1600 nm band, the corresponding value is 3.7 mm. The difference implies a linewidth broadening in the idler band which due to the fact that the linewidth of the idler is slightly broadened by pump.

4.2 Spectroscopic OCT imaging

Fig. 7 shows the spectroscopic OCT imaging result of the anterior segment fish eyeball. Each image was obtained by averaging 10 adjacent frames which are acquired in 0.2 s. Detection range covers a depth of 4 mm. Fig. 7 (A)

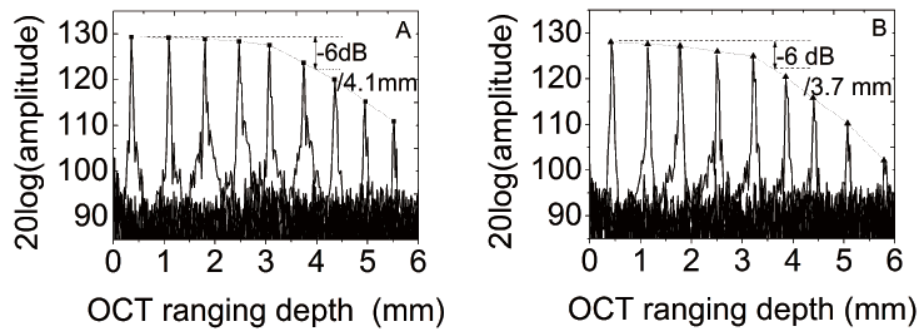


Figure 6. Roll-off characteristics of (A) 1500 nm signal band (B) 1600 nm idler band.

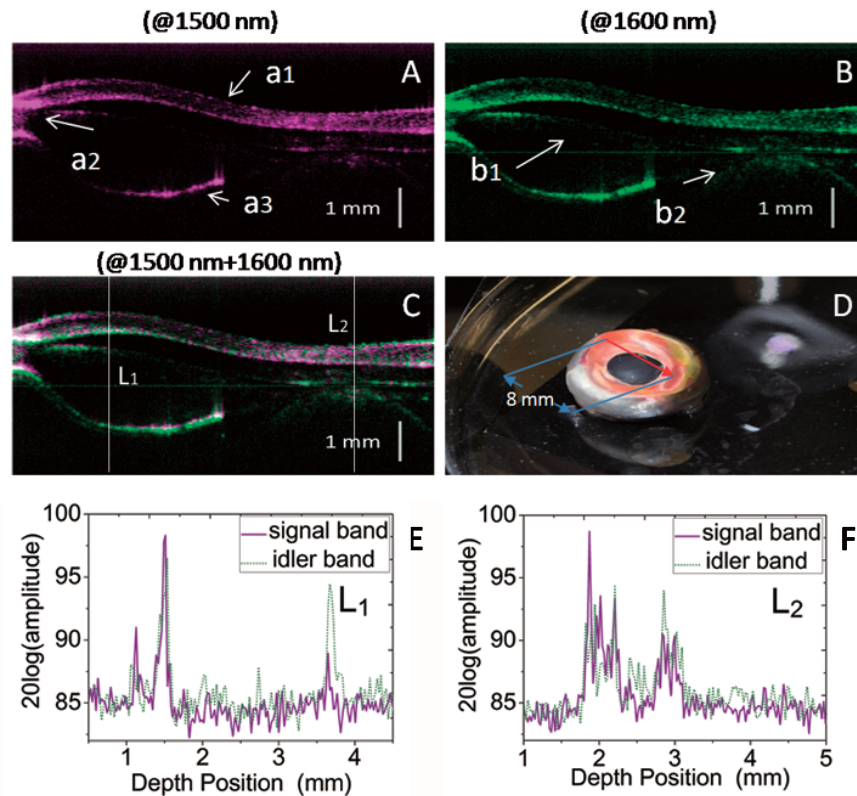


Figure 7. OCT images of a fish eyeball (10 frames averaged). The cornea in anterior segment collapsed during the detached operation. Color encoded (A) signal band/1500nm OCT image and (B) idler band/1600nm OCT image; (C) Combined spectroscopic OCT image; (D) Photo of the experimental sample where the transversal scan covers a range of 8 mm; (E) and (F) Intensity comparisons of two bands at position L_1 and L_2 . a1: cornea (collapsed); a2: angle; a3: iris; b1: anterior chamber; b2: pupil and lens.

and Fig. 7 (B) are color encoded dual-band SOCT images. Fig. 7 (E) and Fig. 7 (F) are two selected A lines where the differences between the bands are quantitatively compared. The scan at 1600 nm shows an enhanced imaging depth especially in deep region of the anterior. This is consistent with the reduced tissue scattering and absorption of hemoglobin in the spectrum range.⁸ The light at 1500 nm is slightly more reflective in the cornea part thus it results in better imaging contrast of the structure. The spectroscopic OCT combines the advantages of two wavelengths and enhances the structure contrast in comparison with OCT image by signal band. In addition, the difference in images at 1500 nm and 1600 nm shows different back scattering and penetration properties at each band. Spectroscopic OCT provides additional information in spectra domain. Although the

resolution of traditional OCT itself is limited to micrometer level, with the help of spectroscopic information, it is promising to realize the breakthrough in molecular imaging by OCT method.

5. CONCLUSION

In conclusion, a high-speed dual wavelength band swept laser source based on an optical parametric amplifier was demonstrated. A dual-band swept-source optical coherence tomography system was implemented to demonstrate the advantage of a second wavelength band for high-quality fast speed spectroscopic OCT. We demonstrate the OPA's characteristics as a dual-band power amplifier and applied the source to achieve the spectroscopic OCT around 1550 nm. Further development on pump power and HNL-DSF may pave the way for ultra-wide band, high resolution spectroscopic OCT system for use in clinical environments.

ACKNOWLEDGMENTS

The work described in this paper was partially supported by the grant from the Research Grants Council of the Hong Kong Special Administrative Region, China (Projects No. HKU 7179/08E and HKU 7183/09E). The authors also acknowledge Sumitomo Electric Industries for providing the HNL-DSF.

REFERENCES

- [1] C. Y. Xu, P. S. Carney, and S. A. Boppart, "Wavelength-dependent scattering in spectroscopic optical coherence tomography," *Optics Express*, 13(14), 5450-5462, 2005.
- [2] F. Spöler, S. Kray, P. Grychtol, B. Hermes, J. Bornemann, M. Först, and H. Kurz, "Simultaneous dual-band ultra-high resolution optical coherence tomography," *Optics Express*, 15(17), 10832-10841, 2007.
- [3] R. Huber, D. C. Adler, and J. G. Fujimoto, "Buffered Fourier domain mode locking: unidirectional swept laser sources for optical coherence tomography imaging at 370,000 lines/s," *Optics Letters*, 31(20), 2975-2977, 2006.
- [4] M. E. Marhic, N. Kagi, T. K. Chiang, and L. G. Kazovsky, "Broadband fiber optical parametric amplifiers," *Optics Letters*, 21(8), 573-575, 1996.
- [5] M. E. Marhic, K. K. Y. Wong, and L. G. Kazovsky, "Wide-band tuning of the gain spectra of one-pump fiber optical parametric amplifiers," *Ieee Journal of Selected Topics in Quantum Electronics*, 10(5), 1133-1141, 2004.
- [6] Y. X. Mao, S. D. Chang, E. Murdock, and C. Flueraru, "Simultaneous dual-wavelength-band common-path swept-source optical coherence tomography with single polygon mirror scanner," *Optics Letters*, 36(11), 1990-1992, 2011.
- [7] G. M. Hale, and M. R. Query, "Optical constants of water in the 200 nm to 200 m wavelength region," *Applied Optics*, 12, 555-563, 1973.
- [8] B. R. Biedermann, W. Wieser, C. M. Eigenwillig, and R. Huber, "Recent developments in Fourier domain mode locked lasers for optical coherence tomography: imaging at 1310 nm vs. 1550 nm wavelength," *Journal of Biophotonics*, 2(67), 357-363, 2009.
- [9] K. H. Y. Cheng, B. A. Standish, V. X. D. Yang, K. K. Y. Cheung, X. Gu, E. Y. Lam, and K. K. Y. Wong, "Wavelength-swept spectral and pulse shaping utilizing hybrid Fourier domain modelocking by fiber optical parametric and erbium-doped fiber amplifiers," *Optics Express*, 18(3), 1909-1915, 2010.